Tonic dendritic GABA release by substantia nigra dopaminergic neurons

DeNard V Simmons[1,5], Oscar Andrés Moreno-Ramos[2,5], Divya D.A. Raj[2,5], Konstantin Kaganovsky [3], Jun Ding [3,5], Rajeshwar Awatramani [2,5], Charles J. Wilson [4], D. James Surmeier [1,5]

[1] Department of Neuroscience, Feinberg School of Medicine, Northwestern University, Chicago, Illinois 60611, USA

[2] Department of Neurology, Feinberg School of Medicine, Northwestern University, Chicago, Illinois 60611, USA,

[3] Department of Neurosurgery, Stanford University School of Medicine, Stanford, CA 94305

[4] Department of Neuroscience, Developmental and Regenerative Biology, University of Texas at San Antonio, San Antonio, Texas 78249

[5] Aligning Science Across Parkinson's (ASAP) Collaborative Research Network, Chevy Chase, MD 20815

*Correspondence:

D. James Surmeier, Department of Neuroscience, Feinberg School of Medicine, Northwestern University

303 East Chicago Avenue, Chicago, IL 60611 USA, j-surmeier@northwestern.edu

Abstract

Recent studies have demonstrated the importance of extrastriatal dopamine release in the emergence of the network dysfunction underlying motor deficits in Parkinson's disease (PD). To better characterize the actions of dopamine on substantia nigra pars reticulata (SNr) GABAergic neurons, optogenetic and electrophysiological tools were used in *ex vivo* mouse brain slices to monitor synaptic transmission arising from globus pallidus externa (GPe) neurons. As predicted by previous work, activation of D2 dopamine receptors (D2Rs) suppressed GABA release evoked by stimulation of GPe axons. However, D2R activation also suppressed a tonic, $GABA_A$ receptor-mediated inhibition of SNr spiking. D2R-mediated inhibition of tonic GABA release led to a roughly 30% increase in SNr spiking rate. Chemogenetic inhibition of GPe terminals or excitation of astrocytes did not affect tonic GABA release in the SNr. In contrast, chemogenetic inhibition of dopaminergic neurons or knocking down the expression of aldehyde dehydrogenase 1A1 (ALDH1A1) blunted tonic GABAergic signaling. Antagonizing D1 dopamine receptors on the terminals of striatonigral neurons also modestly increased SNr spiking. Lastly, in a progressive mouse model of PD targeting dopaminergic neurons, the tonic

inhibition of SNr neurons by GABA release also was lost. Taken together, these observations suggest that dopamine and GABA are co-released by the dendrites of ALDH1A1-expressing dopaminergic neurons that course through the SNr. The co-release of these transmitters could serve to promote movement by making SNr neurons less responsive to phasic activity arising from the indirect pathway circuitry and by lowering basal spiking rates.

Introduction

Parkinson's disease (PD) is the second most common neurodegenerative disease [1, 2]. The cardinal motor symptoms of the disease – bradykinesia and rigidity – are attributable to the degeneration of dopaminergic neurons in the substantia nigra pars compacta (SNc) that innervate the basal ganglia. Although the classical model of the network dysfunction underlying PD motor symptoms emphasizes the importance of the dopaminergic innervation of the striatum (the largest of the basal ganglia nuclei), recent work has demonstrated that other basal ganglia nuclei also are important in the transition to the parkinsonian state, including the substantia nigra pars reticulata (SNr) [3, 4].

From the network standpoint, the SNr is particularly interesting. The principal SNr neurons are autonomously active GABAergic neurons that tonically inhibit motor control circuits in the brainstem and diencephalon [5]. The basal activity of SNr neurons is bidirectionally regulated by synaptic connections with other basal ganglia neurons, including GABAergic neurons in the GPe and striatum (direct pathway spiny projection neurons) and glutamatergic neurons in the subthalamic nucleus (STN) [6, 7]. These synaptic connections are generally thought to be modulated by dopamine through presynaptic G-protein coupled receptors (GPCRs). The dopamine that acts on these receptors is released locally by the dendrites of SNc neurons that course through the SNr [8, 9]. Previous studies have suggested that dopamine released into the SNr suppresses synaptic transmission arising from GPe and STN neurons, while enhancing transmission from direct pathway spiny projection neurons (dSPNs). However, the neuropil in this region is complex, making a definitive assessment of how dopamine modulates these pathways problematic with conventional electrical stimulation methodologies. Optogenetic methods offer a way of surmounting this difficulty, but this approach has not been used to determine how dopamine modulates either GPe or STN input to SNr neurons. Sorting this out in a rigorous way is critical to understanding not only how dopamine modulates SNr activity in the healthy brain, but how this activity goes awry in PD. The potential impact of this local dopaminergic modulation has been driven home by the observation that in parkinsonian MCI-Park mice, restoration of dopaminergic signaling within the SNr alone alleviates open field deficits [10].

Recent work points to another way in which nominally dopaminergic neurons in the SNc might modulate SNr activity. Optogenetic stimulation of genetically defined dopaminergic neurons has

revealed that some of these neurons co-release glutamate and others co-release GABA from their axon terminals [11-13]. It is unclear whether transmitter co-release is a phenomenon limited to axons or whether it extends to the dendrites of SNc dopaminergic neurons.

The goal of the study presented here was to define how dopamine modulates the activity of SNr neurons. The initial experiments utilized optogenetic approaches to characterize how dopamine modulated the release of GABA from GPe synaptic terminals on SNr neurons. These studies were consistent with inferences drawn from previous work that presynaptic D2 dopamine receptors (D2Rs) inhibit phasic release of GABA from GPe terminals. However, these experiments also revealed that D2Rs suppressed a tonic GABAergic inhibition of SNr spiking. This tonic GABAergic signal was traced back to SNc dopaminergic neurons. In part, the tonic GABA release was attributable to D1 dopamine receptor (D1R) facilitated release from direct pathway spiny projection neuron (dSPN) terminals. However, another component was traced to dendritic co-release of dopamine and GABA. This co-release served to promote movement by making SNr neurons less responsive to phasic activity arising from the indirect pathway circuitry and by lowering basal spiking rates. Consistent with this conjecture, the tonic release of GABA was lost in a progressive mouse model of PD that specifically targeted dopaminergic neurons.

Results

D2R agonists inhibited phasic GABA release from GPe terminals

To characterize how dopamine modulated GABA release from GPe terminals, GPe neurons were induced to express the opsin Chronos by injecting an adenoassociated virus (AAV) carrying a synapsin promoter driven expression plasmid with a tdTomato fluorescent protein reporter (see Methods) into the GPe of mice (Fig. 1A). Three to four weeks later, mice were sacrificed, and mesencephalic slices prepared for study. Optogenetic stimulation of GPe axons evoked robust post-synaptic currents in SNr neurons voltage clamped at -60 mV with a Cs^+ containing whole-cell electrode (Fig. 1B). These optically evoked currents were blocked by bath application of the $GABA_A$ receptor ($GABA_AR$) antagonist gabazine (10 µM). To assess dopaminergic modulation of synaptic transmission, the D2R agonist quinpirole (2 µM) was bath applied while optogenetically stimulating GPe axons. Quinpirole reduced the amplitude of the GPe evoked inhibitory postsynaptic currents (IPSCs) by roughly 30% ($p = 0.02$, $n = 5$) (Fig. 1 B, C). Consistent with a presynaptic locus of the modulation, the paired-pulse ratio of GPe evoked IPSCs rose significantly in the presence of quinpirole ($p = 0.02$, $n = 6$) (Fig. 1 D, E).

To assess the impact of this presynaptic modulation on the ability of GPe to modulate the basal spiking of SNr neurons, they were recording in cell-attached mode (to preserve the intracellular environment) and then GPe axons stimulated at 30 Hz for 2 seconds. Initially, this stimulation effectively

suppressed SNr activity, but the efficacy of this inhibition waned with time (Fig. 2A-C). The waning strength of the GPe inhibition is likely attributable to both biologically relevant factors, like depression of GABA release, but also to the limitations posed by the optogenetic methods [14]. As expected, quinpirole attenuated the ability of GPe stimulation to slow the spiking of SNr neurons ($p = 0.02$, $n = 8$) (Fig. 2A-C). Taken together, these results are consistent with the inferences drawn from previous work using electrical stimulation [15].

D2R agonists lowered tonic GABA release

One of the unexpected observations in these experiments was the elevation in the basal spiking rate of SNr neurons with bath application of quinpirole, in the absence of GPe axon stimulation ($p < 0.01$, $n = 8$) (Fig. 3A). The quinpirole-induced elevation in discharge rate was about 50% when monitored in cell-attached mode. Bath application of gabazine (10 µM) increased the basal spiking rate of SNr neurons recorded in cell-attached mode by roughly 25%, suggesting that they were tonically inhibited by activation of $GABA_A$Rs ($p < 0.01$, $n = 10$) (Fig. 3B). These results suggest that quinpirole and gabazine might be acting through a common mechanism – inhibition of tonic GABA release. If this was the case, bath application of gabazine should occlude the modulation of SNr spiking by quinpirole. Indeed, in the presence of gabazine, quinpirole did not significantly modulate SNr spiking rate ($p = 0.13$, $n = 7$) (Fig. 3C).

These results demonstrate that there is a sustained source of GABA that significantly modulates the spiking rate of SNr neurons, and this tonic GABA release is negatively modulated by D2-class receptors. Within the SNr, there are several possible sources of tonic GABA release that might be shaped by D2R signaling (Fig. 3E): GPe terminals, astrocytes, dSPN terminals and SNc dopaminergic neurons. As SNr neurons are not known to express D2-class dopamine receptors, they were excluded as possible sources of tonic GABAergic signaling.

D2R-regulated tonic GABA release was not derived GPe terminals or astrocytes

One potential source of tonic GABA release that might be negatively modulated by D2Rs is the GPe terminal. To test this hypothesis, an AAV carrying a synapsin-driven hM4D (Gi) designer receptor exclusively activated by designer drugs (Gi-DREADD)-tdTomato expression construct was injected into the GPe. Three-four weeks later, mice were sacrificed and *ex vivo* experiments performed. Bath application of the DREADD agonist CNO reduced the amplitude of electrically evoked IPSCs in voltage-clamped SNr neurons ($p = 0.02$, $n = 4$) (Fig. 4A). This modulation was similar in magnitude to that seen in optogenetically evoked IPSCs following D2R stimulation. However, CNO application had no effect on the basal spiking rate of SNr neurons recorded in cell-attached mode, arguing that GPe terminals were not contributing to tonic GABA release ($p = 0.19$, $n = 5$) (Fig. 4B).

Many astrocytes express D2Rs [16-18]. Moreover, in some regions of the brain, astrocytes are known to release GABA [19]. Astrocytic GABA release is thought to occur through bestrophin1 channels in response to an elevation in intracellular Ca^{2+} concentration [20]. To test if astrocytes in the SNr mediate tonic GABA, an AAV carrying a plasmid in which a glial fibrillary acidic protein (GFAP) promoter fragment controlled expression of an excitatory hM3 (Gq) DREADD construct was stereotaxically injected into the SNr of mice. These vectors have been used to chemogenetically elevate intracellular Ca^{2+} in astrocytes [21] (Fig. 5A). Three-four weeks after the AAV injection, mice were sacrificed and brain slices prepared. In these slices, bath application of the DREADD agonist CNO elevated the basal spiking rate of SNr neurons recorded in cell-attached mode ($p = 0.03$, $n = 8$) (Fig. 5B). In line with the notion that astrocytes were exciting (not inhibiting) SNr neurons, bath application of the bestrophin 1 inhibitor NPPB decreased SNr spiking rate ($p = 0.03$, $n = 6$) (Fig. 5C).

Dendritically released dopamine enhanced tonic GABA release from dSPN terminals

In addition to suppressing GABA release from GPe terminals, dendritically released dopamine can facilitate GABA release from dSPN terminals invested with D1Rs [22-24]. Although previous work has focused on spike-evoked GABA release, it is also possible that D1R stimulation promotes tonic GABA release from these terminals. Thus, by suppressing dendritic dopamine release, D2R stimulation might dis-facilitate GABA release from dSPN terminals. To test this possibility, a D1R antagonist was bath applied while monitoring SNr spike rate. Bath application of SCH39166 (2 μM) did indeed significantly elevate SNr spiking rate ($p = 0.02$, $n = 12$) (Fig. S1), but much less than that produced by the D2R agonist – arguing that there was another source of tonic GABA release in the SNr.

SNc dopaminergic neurons directly contributed to tonic GABA release

Another possible source of tonic GABA release is SNc dopaminergic neuron. As mentioned above, SNc dopaminergic neurons co-release dopamine and GABA, at least from their striatal axons. Moreover, the somatodendritic region of these neurons is richly invested with D2Rs that are coupled to Kir2 K^+ channels that suppress spiking and dopamine release [16, 25]. The release of GABA from the axons of dopaminergic neurons is inhibited by D2Rs as well [26]. One of the enzymes thought to be important in the production of releasable GABA is aldehyde dehydrogenase 1α1 (ALDH1A1) [27]. To assess the extent to which ALDH1A1 dendrites innervate the SNr, mice expressing Cre recombinase in ALDH1A1+ (Aldh1a1-2A-iCre) neurons were crossed with mice expressing the recombinase FlpO under the control of the dopamine transporter promoter (DAT-2A-Flpo). These mice were then injected with AAV8 HSyn-Con/Fon-YFP, and AAV8 Ef1a-Coff/Fon-mCherry viruses. 4 weeks after the injection, mice were sacrificed for histological analysis. In tissue from these mice, ALDH1A1+ dopaminergic neurons were marked by EYFP expression, whereas ALDH1A1- dopaminergic neurons were marked with mCherry. In both rostral and caudal regions, the dendrites of ALDH1A1+ dopaminergic neurons

coursed through much of dorsoventral extent of SNr, providing an anatomical substrate for the distributed release of GABA (Fig. 6A, B) [9, 28].

As a first test of the role of ALDH1A1 in generating the tonic GABA signal, a viral knockdown strategy was used. The SN of mice expressing Cre recombinase under control of the DAT promoter (DAT-IRES-Cre), were stereotaxically injected with an AAV carrying a FLEX ALDH1A1 shRNA expression construct with an mCherry reporter (Fig. 6C) [27]. Two weeks later, mice were sacrificed and brain slices prepared. In *ex vivo*, cell-attached recordings from SNr neurons, the basal spiking rate was significantly higher than in controls ($p < 0.001$, $n = 18$ control / 15 shRNA) (Fig. 6D). Moreover, bath application of gabazine did not change the basal spiking rate of SNr neurons from ALDH1A1 shRNA treated mice ($p = 0.10$, $n = 15$) (Fig. 6E).

To provide an orthogonal test of the hypothesis that ALDH1A1 was driving GABA synthesis, a pharmacological approach was used. First, the ALDH1A1 inhibitor disulfiram (10 µM) was bath applied to control slices and then the effect of gabazine on basal spiking rate monitored. Disulfiram blocked the effect of gabazine ($p = 0.80$, $n = 5$) (Fig. 6G). Second, another inhibitor of ALDH1A1 N,N-diethylaminobenzaldehyde (DEAB, 10 µM) was bath applied and the effect of gabazine on basal spiking monitored. As with disulfiram, gabazine had no effect on DEAB-exposed SNr neurons ($p = 0.19$, $n = 5$) (Fig. 6H).

An alternative interpretation of these results is that disruption of ALDH1A1 function impairs dendritic dopamine release. Although ALDH1A1 is involved in the degradation of dopamine (not its synthesis) [29], this possibility was tested by examining striatal dopamine release using fast scan voltammetry in *ex vivo* brain slices from control and *ALDH1A1* knockout mice [27]. As expected, deletion of *ALDH1A1* did not affect dopamine release (Fig. S2).

As a final test of the hypothesis that SNc dopaminergic neurons were the source of tonic GABA release in the SNr, a chemogenetic approach was used. The SN of DAT-Cre mice was stereotaxically injected with an AAV carrying a FLEX construct coding for the glycine pharmacologically selective actuator module (PSAM-L141-Y115F-GlyR). Three weeks later, mice were sacrificed and mesencephalic slices prepared. Histological analysis of the mesencephalon of these mice showed good overlap of tyrosine hydroxylase immunoreactivity and the PSAM reporter (Fig. 7A, B). In principle, once activated, the glycine PSAM should modestly hyperpolarize SNc dopaminergic neurons and decrease Ca^{2+}-dependent GABA release (Fig. 7C). In cell attached patch recordings from PSAM-expressing neurons, bath application of the pharmacologically selective effector molecule (PSEM) uPSEM817 tartate (0.5 µM) modestly reduced the tonic spiking of SNc dopaminergic neurons ($p = 0.03$, $n = 10$) (Fig. 7D). Furthermore, as predicted, bath application of the PSEM also significantly increased

SNr spiking rate, consistent with the hypothesis that autonomously active SNc dopaminergic neurons were the source of tonic GABAergic inhibition ($p = 0.02$, $n = 8$) (Fig. 7E).

Tonic GABA release was lost in a mouse model of PD

In the MCI-Park model of PD, the emergence of parkinsonism parallels the down-regulation of the dopaminergic phenotype in the somatodendritic region of SNc dopaminergic neurons [10]. This phenotypic down-regulation is accompanied by a loss of dopamine release in the SNr. If dopamine and GABA were co-released by dendrites, tonic GABA release also should be down-regulated in parkinsonian MCI-Park mice. Indeed, in contrast to littermate controls (Fig. 8A), bath application of gabazine failed to increase the spiking rate of SNr neurons recorded in *ex vivo* slices from P60-70 MC1-Park mice ($p = 0.69$, $n = 7$) (Fig. 8B).

Discussion

There are three conclusions that can be drawn from the studies presented. First, activation of D2-class dopamine receptors suppressed optogenetically-induced, phasic release of GABA from GPe axon terminals synapsing on SNr neurons. Second, activation of D2-class dopamine receptors also suppressed a tonic GABAergic inhibition of autonomous SNr spiking. Although a small component of this tonic GABA release was attributable to dendritically-released dopamine facilitating GABA release from dSPN terminals, the principal component of this tonic signaling was attributable to dendritic release of GABA from SNc dopaminergic neurons. Lastly, in a progressive model of PD, tonic GABAergic signaling in the SNr was lost in parallel with the loss of dopaminergic signaling. These results suggest that a subset of SNc dopaminergic neurons co-release dopamine and GABA from their dendrites, as has been recently reported for their axons in the striatum. The concomitant loss of dendritic release of dopamine and GABA in SNr may be a key step in the emergence of the network pathophysiology underlying the parkinsonism.

Presynaptic D2-class dopamine receptors suppressed GABA release by GPe terminals

GPe GABAergic projection neurons form large perisomatic synapses on SNr neurons [30]. Previous studies using electrical stimulation of fiber tracks, in combination with pharmacological and electrophysiological methods in ex vivo brain slices, had inferred that presynaptic D2-class dopamine receptors inhibited the release of GABA from GPe terminals on SNr neurons [15]; this modulation was attributed to a combination of D_3 and D_4 dopamine receptors based upon pharmacological criteria. Given the inability of electrical stimulation to activate specific neurons and the potential heterogeneity of GABAergic inputs to SNr neurons, optogenetic approaches were used here to definitively test this inference. Although the type of D2-class receptor involved was not addressed in our studies, they do

demonstrate that GPe terminals possess D2-class receptors that robustly suppress GABA release at synapses on SNr neurons.

Tonic GABAergic signaling in SNr was largely attributable to dendritic release by SNc dopaminergic neurons

In addition to inhibiting optogenetically evoked GABA release from GPe terminals, the D2-class receptor agonist quinpirole suppressed a tonic, $GABA_AR$ mediated inhibition of spontaneous SNr neuron spiking. This tonic GABA current was not diminished by chemogenetic inhibition of GPe terminals or astrocytes, pointing to an alternative source. Our experiments identified two other sources. One source of tonic GABA signaling appeared to be the synaptic terminals of dSPNs, as antagonizing D1Rs, which facilitate dSPN terminal GABA release [22-24], modestly elevated the basal spiking rate of SNr neurons. As dendritic release of dopamine is negatively modulated by D2 autoreceptor signaling [16, 25], quinpirole should dis-facilitate tonic GABA release from dSPN terminals. However, the modal change in spiking rate produced by antagonizing D1Rs was small (~10%) compared to that produced by D2R agonist quinpirole (~50%)

Several observations suggest that the principal source of tonic GABA signaling in SNr was ALDH1A1-expressing SNc dopaminergic neurons. These dopaminergic neurons reside near the border between SNc and SNr and have dendrites that course through much, if not all, the SNr. As for axonal release, dendritic dopamine release is Ca^{2+} dependent and negatively modulated by D2R autoreceptor signaling [16, 25]. Recent work has shown that a subset of SNc dopaminergic neurons co-release GABA from their axon terminals in the striatum [13, 26, 27]. Our work suggests that there also is co-release of dopamine and GABA from the dendrites of dopaminergic neurons, as modest chemogenetic inhibition of SNc dopaminergic neurons reduced tonic GABAergic inhibition of SNr neurons. Although relative contributions of GABA uptake from the extracellular space and intracellular synthesis of GABA by an ALDH1A1-dependent mechanism to axonal release remain the subject of study [27, 31], disrupting ALDH1A1 function clearly diminished tonic GABAergic signaling in the SNr. Degrading *ALDH1A1* mRNA with a virally delivered siRNA or pharmacologically inhibiting ALDH1A1 [27] occluded the effect of gabazine on SNr spiking. ALDH1A1 deletion did not affect dopamine release by SNc neurons, arguing that the effect of disrupting ALDH1A1 function on tonic GABA signaling was not an indirect consequence of suppressing dopamine release in the SNr. Given that many of the SNc dopaminergic neurons with dendrites investing the SNr did not express ALDH1A1, it is possible that GABA co-release is a property of only a subset of SNc dopaminergic neurons or that the mechanisms governing co-release are varied.

Coordinated modulation of SNr by dendritic co-release of GABA and DA

Although the classical model of network dysfunction argues that striatal dopamine depletion is both necessary and sufficient for the emergence of the cardinal motor symptoms of PD, there is a growing body of evidence that extrastriatal signaling by SNc neurons plays a critical role [32-34]. For example, in otherwise healthy rodents, disrupting dopaminergic signaling within the SNr promotes the emergence of irregular, burst mode spiking in principal neurons and parkinsonism [15, 35], much like global dopamine depletion produced by 6-OHDA lesions [36-39]. Similar alterations the pattern of SNr or globus pallidus interna (GPi) spiking have been observed in primate models of PD [40]. Consistent with the role of SNr dopaminergic signaling in parkinsonism, recent work in a progressive mouse model of PD has shown that boosting conversion of levodopa to dopamine within the SNr effectively alleviates bradykinesia [10]. This observation aligns with earlier work suggesting that the SNr is a key site of levodopa action [41].

Even though the emergence of the bursting pattern of activity is commonly attributed to altered dopaminergic modulation of afferent input to SNr neurons [15, 42], it is mimicked by local inhibition of $GABA_A$Rs [43] - suggesting that tonic GABAergic and dopaminergic signaling could work in concert to regularize SNr activity and promote normal movement. Indeed, tonic GABAergic signaling in SNr was lost in parkinsonian MCI-Park mice. Precisely when in the evolution of the dysfunction of SNc dopaminergic neurons tonic GABA release becomes impaired remains to be determined; but recent work with a toxin model suggests that loss of GABA release in the striatum precedes deficits in dopamine release [44].

The precise mechanisms controlling the emergence of burst spiking in SNr neurons in PD models remain to be resolved. The fact that bursting is observed in ex vivo preparations where patterned synaptic input is lost argues that cell-intrinsic mechanisms governing the autonomous activity of SNr neurons are involved. That said, it is also possible that *in vivo* there is an interaction between network pathophysiology and intrinsic processes that drive aberrant SNr activity. Tonic $GABA_A$R activation might provide an outward current that counter-balances the constitutively active inward currents driving autonomous pacemaking. In this way, slowing intrinsically generated activity could make SNr neurons more responsive to extrinsic synaptic input conveying information about movement, particularly that arising from distal, dSPN GABAergic synapses. In the parkinsonian state, the loss of tonic GABAergic input and the disinhibition of peri-somatic GPe GABAergic synapses could lead an aberrant elevation in the influence of GPe on SNr patterning and pathological rhythmicity [45-48]. In alignment with this hypothesis, chemogenetic inhibition of SNr neurons alleviates parkinsonian motor disability in an animal model [49].

Methods

Animals

All housing, breeding and procedures were performed according to the Northwestern University Animal Studies committee and in accordance with the National Institutes of Health Guide for the Care and Use of Laboratory Animals. Mice were group housed with food and water provided ad libitum under a 12 h-12 h light-dark cycle and temperatures of 65-75 °F with 40-60% humidity. Male and female mice were used for experiments. No significant differences were observed between both groups. We obtained *DAT-Cre* mice (B6.SJL-Slc6a3$^{tm1.1(cre)Bkmn}$/J) from the Jackson Laboratories. We obtained C57BL/6J and PV-Cre mice (B6.129P2-Pvalb$^{tm1(cre)Arbr}$/J) from the Jackson Laboratories. MC1-Park mice (DAT-Cre x Ndufs2 $^{-/-}$) were bred in house [10]. Aldh1a1-2A-iCre/Dat-2A-Flpo adult mice (P>60) were generated in house.

Stereotaxic injections

Mice were anaesthetized using an isoflurane precision vapourizer (SomnoSuite - Kent Scientific) and placed in a stereotaxic frame (David Kopf Instruments) with a Cunningham adaptor (Harvard Apparatus) to maintain anesthesia delivery throughout surgery. After exposing the skull, a small hole was bored with a micro drill bit and 200 nl of viral vector was delivered through a glass micropipette (Drummond Scientific Company) pulled on a Sutter P-97 puller. The SNr was targeted at the following coordinates (mm): anterioposterior (AP) = -3.40, mediolateral (ML) = 1.41 and dorsoventral (DV) = -4.45 (all (AP, ML, DV) relative to the bregma). For ALDH-shRNA experiments, the SNc was targeted at the following coordinates: AP = -3.0, ML = 1.2, DV = 4.2. For the DAT-FLP/ALDH1A1-Cre labeling experiments, the SNc was targeted at the following coordinates: AP = -3.16, ML = -1.5, DV = 4.00, and a volume of 300nL was injected of a mix 1:1 of AAV8 HSyn-Con/Fon-YFP (titer:2.4x10^{13}GC/mL) and AAV8 Ef1a-Coff/Fon-mCherry (titer: 2.2X10^{13}GC/mL). The GP was targeted at the following coordinates: AP = -0.34, ML = 1.81, DV = 3.61, and AP = -0.82, ML = 2.33, DV = 3.72.

Source of coordinates and diagrams: Allen Mouse Brain Atlas

Recombinant AAV vectors

The following AAV viruses were used in this study: AAV9-hSyn-hM4Di-mCherry (Addgene; RRID:Addgene_50475), AAV9-hSyn-DIO-hM4Di-mCherry (Addgene; RRID:Addgene_44362), AAV9-Ef1a-DIO-PSAM-L141F-Y115F-GlyR-2A-FusionRed (Virovek), AAV2/5-GfAABC$_1$D-hM3Dg-mCherry (Addgene; RRID:Addgene_50478), AAV-CMV-Aldh1a1-shRNA (Stanford, [27]), AAV8 HSyn-Con/Fon-

YFP (addgene: #55650-AAV8, titer:2.4x10^{13}GC/mL) and AAV8 Ef1a-Coff/Fon-mCherry (addgene: #137134-AAV8, titer: 2.2X10^{13}GC/mL)

Ex vivo brain slice preparation

Mice were anaesthetized with a mixture of ketamine (50 mg kg^{-1}) and xylazine (4.5 mg kg-1) then transcardially perfused with ice-cold, oxygenated modified artificial cerebrospinal fluid (aCSF) containing 210 mM sucrose, 2.5 mM KCl, 1.25 mM NaH_2PO_4, 25 mM $NaHCO_3$, 0.5 mM $CaCl_2$, 10 mM $MgSO_4$ and 10 mM glucose, pH 7.3 (315–320 mOsm $l^{-1)}$. Once perfused, the brain was rapidly removed and either sagittal or coronal slices containing the SNr (thickness, 240 µm) were sectioned using a vibratome (VT1200S Leica Microsystems). Brain slices were incubated in oxygenated modified aCSF containing 124 mM NaCl, 4.5 mM KCl, 25 mM $NaHCO_3$, 1.25 mM NaH_2PO_4, 1.2 mM $CaCl_2$, 1.8 mM $MgCl_2$ and 10 mM glucose at 34 °C for 30 min, then at room temperature for another 30 min before the experiments. All solutions were pH 7.4, 310-320 mOsm l^{-1} and were continually bubbled with 95%O_2/5% CO_2. Experiments were performed at 32-33 °C.

Immunohistochemistry

After recording, brain slices were fixed in 4% PFA for 15 min to preserve the epitope for TH antibody staining. Rabbit-anti TH (Millipore sigma AB152) was used as primary to label dopamine neurons in fixed tissue. Aldh1a1-2A-iCre/Dat-2A-Flpo adult mice were perfused with cold 4% PFA in 1X PBS pH 7.4, the brains were dissected and fixed overnight in the same solution, cryoprotected in 30% sucrose in PBS, sectioned at 25 µm using a freezing microtome, and stored at –20°C in cryoprotectant solution. For immunofluorescence on free-floating sections, tissue was rinsed 4 times in 1XPBS, pH 7.4, blocked for a minimum of 2 hours in 5% donkey serum, 0.3% Triton X-100 in 1XPBS, pH7.4; and incubated overnight at 4°C with primary antibodies diluted in blocking solution: Rat anti-mCherrry (cat. no. M11217; Invitrogen; 1:250), chicken anti-GFP (cat. no. ab13970; Abcam; 1:250), sheep anti-TH (cat. no. P60101-0; Pel-Freez; 1:250). Sections were rinsed in PBS plus 0.05% Tween-20 solution and incubated with secondary antibodies (from Invitrogen: Alexa 647 donkey anti-sheep, A-31571; Jackson ImmunoResearch Laboratories: Alexa 488 donkey anti-chicken, 162189 and Alexa 555 donkey anti-Rat, 712-165-155), diluted 1:250 in blocking solution and counterstained with DAPI (Sigma), rinsed in PBS plus 0.05% Tween20, and finally coverslipped with Gelvatol.

Fast-scan cyclic voltammetry (FSCV)

Extracellular dopamine release was monitored by fast-scan cyclic voltammetry recordings performed in 300 µm coronal sections of dorsal striatum using carbon-fiber microelectrodes (7 µm diameter carbon fiber extending 50~100 µm beyond the tapered glass seal). Cyclic voltammograms were measured with a triangular potential waveform (-0.4 to +1.3 V vs Ag/AgCl reference electrode, 400 V/s scan rate, 8.5 ms waveform width) applied at 100 ms intervals. The carbon fiber microelectrode was held at -0.4 V between scans. Cyclic voltammograms were background-subtracted by averaging 10 background scans. Each striatal hemisphere was recorded in both dorsal lateral and dorsal medial striatum, and the order of recording was counterbalanced across slices. Dopaminergic axon terminals were stimulated locally (100-200µm from carbon fiber) with an electrode at 100 µA. First, each recording site received 2 electrical stimulations separated by 15seconds, after 2 minutes of recovery time, the same site received a train of stimulation (5 pulses at 25Hz). Evoked dopamine release and subsequent oxidation current was detected and monitored using the TarHeel CV system. Changes in dopamine concentration by optical stimulation were quantified by plotting the peak oxidation current of the voltammogram over time. Carbon fiber microelectrode was calibrated at the end of each day of experiments to convert oxidation current to dopamine concentration using 10 µM dopamine in ACSF.

Analysis and statistics

Electrophysiology data were generally analyzed using Clampfit 10.3 software (Molecular Devices; https://www.moleculardevices.com/products/axon-patch-clamp-system/acquisition-and-analysis-software/pclamp-software-suite. Data are summarized using box plots showing median values, first and third quartiles, and range, unless otherwise specified. Statistical analysis was performed with Mathematica 13 (Wolfram; https://www.wolfram.com/mathematica/?source=nav) and GraphPad Prism 8 (GraphPad Software; https://www.graphpad.com/). Probability threshold for statistical significance was $P < 0.05$.

Table for Materials & Methods

Reagent or Resource	Source	Identifier
Experimental Models: Organisms/Strains		
C57BL/6J	Jackson Laboratories	RRID:IMSR JAX:000664
DAT-Cre x Ndufs2 $^{-/-}$	Available at Jackson Laboratories, strain bred in house for these experiments	RRID:IMSR_JAX:036313
Ndufs2^{fl}	Dr. José López-Barneo (Universidad de Sevilla)	MGI:J:322308
DAT-Cre (B6.SJL-Slc6a3$^{tm1.1(cre)Bkmn}$/J)	Jackson Laboratories	RRID:IMSR_JAX:006660
PV-Cre mice	Jackson Laboratories	RRID:MGI:5504648

(B6.129P2-Pvalb$^{tm1(cre)Arbr}$/J)		
Materials		
AAV9-hSyn-hM4Di-mCherry	Addgene	RRID:Addgene_50475
AAV9-hSyn-DIO-hM4Di-mCherry	Addgene	RRID:Addgene_44362
AAV9-Ef1a-DIO-PSAM-L141F-Y115F-GlyR-2A-FusionRed	Virovek	No RRID available
AAV2/5-GfAABC$_1$D-hM3Dg-mCherry	Addgene	RRID:Addgene_50478
Rabbit-anti TH antibody	Millipore-Sigma	Millipore Cat# AB152, RRID:AB_390204
AAV-CMV-Aldh1a1-shRNA	Stanford: Virus generated by Jun Ding Lab; Plasmid provided by Lu Chen Lab	No RRID available
AAV8 HSyn-Con/Fon-YFP	Addgene	RRID:Addgene_55650
AAV8 Ef1a-Coff/Fon-mCherry	Addgene	RRID:Addgene_137134
Software and Algorithms		
Mathematica 13	Wolfram; https://www.wolfram.com/mathematica/?source=nav	RRID:SCR_014448
Clampfit v 10.3	Molecular Devices; https://www.moleculardevices.com/products/axon-patch-clamp-system/acquisition-and-analysis-software/pclamp-software-suite	RRID:SCR_011323
GraphPad Prism v.8	URL: http://www.graphpad.com/	RRID:SCR_002798
Allen Mouse Brain Common Coordinate Framework	URL: https://atlas.brain-map.org/	RRID:SCR_020999
Methods		
Protocol Title	Section in Methods	DOI (Protocols.io)
Mouse Stereotaxic Surgeries for Intracranial Viral Injection V.1	Stereotaxic viral injections	**dx.doi.org/10.17504/protocols.io.81wgby191vpk/v1**
Preparation of ex-vivo brain slices	Ex vivo brain slice preparation	dx.doi.org/10.17504/protocols.io.dm6gp328jvzp/v2

for physiology experiments V.2		
Ex vivo mouse brain patch clamp recordings combined with optogenetic stimulation	Slice recording and optogenetic stimulation	dx.doi.org/10.17504/protocols.io.5qpvokxp9l4o/v1
Immunofluorescence for confocal imaging after slice recording	Immunohistochemistry	dx.doi.org/10.17504/protocols.io.6qpvr8xmolmk/v1
Fast scan cyclic voltammetry	FSCV	fast-scan-cyclic-voltammetry-kxygx9py4g8j/v1
Datasets and Code		
Zenodo Name	Description	DOI
Data and Images for Tonic dendritic GABA release by substantia nigra dopaminergic neurons	Data sets and Images for Figures	10.5281/zenodo.10850897
Mathematica code for Tonic dendritic GABA release by substantia nigra dopaminergic neurons	Mathematica code used to generate datasets	10.5281/zenodo.10855007

Acknowledgments

We thank Dr. Bal Khakh from the UCLA David Geffen School of Medicine for his insights on the astrocyte experiments. The study was supported by a fellowship from the Bumpus Foundation (DS), and grants to DJS from the JPB Foundation and Aligning Science Across Parkinson's (ASAP) Grant # 020551.

References

1. Beitz, J.M., *Parkinson s disease a review.* Frontiers in Bioscience, 2014. **S6**(1): p. 65-74.
2. McGregor, M.M. and A.B. Nelson, *Circuit Mechanisms of Parkinson's Disease.* Neuron, 2019. **101**(6): p. 1042-1056.
3. Smith, Y. and J.Z. Kieval, *Anatomy of the dopamine system in the basal ganglia.* Trends Neurosci, 2000. **23**(10 Suppl): p. S28-33.
4. Mallet, et al., *Cellular and Synaptic Dysfunctions in Parkinson's Disease: Stepping out of the Striatum.* Cells, 2019. **8**(9): p. 1005.
5. McElvain, L.E., et al., *Specific populations of basal ganglia output neurons target distinct brain stem areas while collateralizing throughout the diencephalon.* Neuron, 2021. **109**(10): p. 1721-1738.e4.
6. Albin, R.L., A.B. Young, and J.B. Penney, *The functional anatomy of basal ganglia disorders.* Trends in Neurosciences, 1989. **12**(10): p. 366-375.
7. Cui, G., et al., *Concurrent activation of striatal direct and indirect pathways during action initiation.* Nature, 2013. **494**(7436): p. 238-42.
8. Damier, P., et al., *The substantia nigra of the human brainI. Nigrosomes and the nigral matrix, a compartmental organization based on calbindin D28K immunohistochemistry.* Brain, 1999. **122**(8): p. 1421-1436.
9. Rice, M.E. and J.C. Patel, *Somatodendritic dopamine release: recent mechanistic insights.* Philosophical transactions of the Royal Society of London. Series B, Biological sciences, 2015. **370**(1672): p. 20140185.
10. González-Rodríguez, P., et al., *Disruption of mitochondrial complex I induces progressive parkinsonism.* Nature, 2021. **599**(7886): p. 650-656.
11. Chuhma, N., et al., *Dopamine neurons mediate a fast excitatory signal via their glutamatergic synapses.* J Neurosci, 2004. **24**(4): p. 972-81.
12. Stuber, G.D., et al., *Dopaminergic terminals in the nucleus accumbens but not the dorsal striatum corelease glutamate.* J Neurosci, 2010. **30**(24): p. 8229-33.
13. Tritsch, N.X., J.B. Ding, and B.L. Sabatini, *Dopaminergic neurons inhibit striatal output via non-canonical release of GABA.* Nature, 2012. **490**(7419): p. 262-266.
14. Lin, J.Y., *A user's guide to channelrhodopsin variants: features, limitations and future developments.* Exp Physiol, 2011. **96**(1): p. 19-25.
15. Aceves, J.d.J., et al., *Dopaminergic Presynaptic Modulation of Nigral Afferents: Its Role in the Generation of Recurrent Bursting in Substantia Nigra Pars Reticulata Neurons.* Frontiers in System Neuroscience, 2011. **5**: p. 6.
16. Beckstead, M.J., et al., *Vesicular dopamine release elicits an inhibitory postsynaptic current in midbrain dopamine neurons.* Neuron, 2004. **42**(6): p. 939-46.
17. Bal, A., et al., *Evidence for dopamine D2 receptor mRNA expression by striatal astrocytes in culture: in situ hybridization and polymerase chain reaction studies.* Brain Res Mol Brain Res, 1994. **23**(3): p. 204-12.

18. Qiu, J., et al., *Sinomenine activates astrocytic dopamine D2 receptors and alleviates neuroinflammatory injury via the CRYAB/STAT3 pathway after ischemic stroke in mice.* J Neuroinflammation, 2016. **13**(1): p. 263.
19. Liu, J., et al., *Astrocytes: GABAceptive and GABAergic Cells in the Brain.* Frontiers in Cellular Neuroscience, 2022. **16**: p. 892497.
20. Park, H., et al., *Bestrophin-1 Encodes for the Ca2+-Activated Anion Channel in Hippocampal Astrocytes.* The Journal of Neuroscience, 2009. **29**(41): p. 13063-13073.
21. Khakh, B.S. and B. Deneen, *The Emerging Nature of Astrocyte Diversity.* Annual Review of Neuroscience, 2019. **42**(1): p. 187-207.
22. Floran, B., et al., *Activation of D1 dopamine receptors stimulates the release of GABA in the basal ganglia of the rat.* Neuroscience Letters, 1990. **116**(1-2): p. 136-140.
23. Radnikow, G. and U. Misgeld, *Dopamine D1 receptors facilitate GABAA synaptic currents in the rat substantia nigra pars reticulata.* J Neurosci, 1998. **18**(6): p. 2009-16.
24. Chuhma, N., et al., *Functional connectome of the striatal medium spiny neuron.* J Neurosci, 2011. **31**(4): p. 1183-92.
25. Lacey, M.G., N.B. Mercuri, and R.A. North, *Dopamine acts on D2 receptors to increase potassium conductance in neurones of the rat substantia nigra zona compacta.* J Physiol, 1987. **392**: p. 397-416.
26. Zych, S.M. and C.P. Ford, *Divergent properties and independent regulation of striatal dopamine and GABA co-transmission.* Cell Reports, 2022. **39**(7): p. 110823.
27. Kim, J.-I., et al., *Aldehyde dehydrogenase 1a1 mediates a GABA synthesis pathway in midbrain dopaminergic neurons.* Science, 2015. **350**(6256): p. 102-106.
28. Damier, P., et al., *The substantia nigra of the human brainII. Patterns of loss of dopamine-containing neurons in Parkinson's disease.* Brain, 1999. **122**(8): p. 1437-1448.
29. Goldstein, D.S., et al., *Determinants of buildup of the toxic dopamine metabolite DOPAL in Parkinson's disease.* J Neurochem, 2013. **126**(5): p. 591-603.
30. Smith, Y. and J.P. Bolam, *The output neurones and the dopaminergic neurones of the substantia nigra receive a GABA-containing input from the globus pallidus in the rat.* J Comp Neurol, 1990. **296**(1): p. 47-64.
31. Melani, R. and N.X. Tritsch, *Inhibitory co-transmission from midbrain dopamine neurons relies on presynaptic GABA uptake.* Cell Reports, 2022. **39**(3): p. 110716.
32. Zhai, S., et al., *Distributed dopaminergic signaling in the basal ganglia and its relationship to motor disability in Parkinson's disease.* Curr Opin Neurobiol, 2023. **83**: p. 102798.
33. Robertson, H.A., *Synergistic interactions of D1- and D2-selective dopamine agonists in animal models for Parkinson's disease: sites of action and implications for the pathogenesis of dyskinesias.* Can J Neurol Sci, 1992. **19**(1 Suppl): p. 147-52.
34. Wichmann, T., *Changing views of the pathophysiology of Parkinsonism.* Mov Disord, 2019. **34**(8): p. 1130-1143.
35. Cáceres-Chávez, V.A., et al., *Acute dopamine receptor blockade in substantia nigra pars reticulata: a possible model for drug-induced Parkinsonism.* Journal of Neurophysiology, 2018. **120**(6): p. 2922-2938.
36. Lobb, C.J. and D. Jaeger, *Bursting activity of substantia nigra pars reticulata neurons in mouse parkinsonism in awake and anesthetized states.* Neurobiol Dis, 2015. **75**: p. 177-85.

37. Murer, M.G., et al., *Substantia nigra pars reticulata single unit activity in normal and 60HDA-lesioned rats: effects of intrastriatal apomorphine and subthalamic lesions.* Synapse, 1997. **27**(4): p. 278-93.
38. Rohlfs, A., et al., *Hemispheric asymmetries in spontaneous firing characteristics of substantia nigra pars reticulata neurons following a unilateral 6-hydroxydopamine lesion of the rat nigrostriatal pathway.* Brain Res, 1997. **761**(2): p. 352-6.
39. Wang, Y., et al., *Changes in firing rate and pattern of GABAergic neurons in subregions of the substantia nigra pars reticulata in rat models of Parkinson's disease.* Brain Res, 2010. **1324**: p. 54-63.
40. Wichmann, T., et al., *Comparison of MPTP-induced changes in spontaneous neuronal discharge in the internal pallidal segment and in the substantia nigra pars reticulata in primates.* Exp Brain Res, 1999. **125**(4): p. 397-409.
41. Robertson, G.S. and H.A. Robertson, *Evidence that the substantia nigra is a site of action for l-DOPA.* Neuroscience Letters, 1988. **89**(2): p. 204-208.
42. Ibanez-Sandoval, O., et al., *Control of the subthalamic innervation of substantia nigra pars reticulata by D1 and D2 dopamine receptors.* J Neurophysiol, 2006. **95**(3): p. 1800-11.
43. Ibanez-Sandoval, O., et al., *Bursting in substantia nigra pars reticulata neurons in vitro: possible relevance for Parkinson disease.* J Neurophysiol, 2007. **98**(4): p. 2311-23.
44. Kim, H.J., et al., *GABAergic-like dopamine synapses in the brain.* Cell Rep, 2023. **42**(10): p. 113239.
45. Nambu, A. and Y. Tachibana, *Mechanism of parkinsonian neuronal oscillations in the primate basal ganglia: some considerations based on our recent work.* Front Syst Neurosci, 2014. **8**: p. 74.
46. Crompe, B., et al., *The globus pallidus orchestrates abnormal network dynamics in a model of Parkinsonism.* Nat Commun, 2020. **11**(1): p. 1570.
47. Dong, J., et al., *Connectivity and Functionality of the Globus Pallidus Externa Under Normal Conditions and Parkinson's Disease.* Front Neural Circuits, 2021. **15**: p. 645287.
48. Mamad, O., et al., *Dopaminergic control of the globus pallidus through activation of D2 receptors and its impact on the electrical activity of subthalamic nucleus and substantia nigra reticulata neurons.* PLoS One, 2015. **10**(3): p. e0119152.
49. Delgado-Zabalza, L., et al., *Targeting parvalbumin-expressing neurons in the substantia nigra pars reticulata restores motor function in parkinsonian mice.* Cell Rep, 2023. **42**(10): p. 113287.

Figure legends

Figure 1. Optically Evoked GPe mediated IPSCs are depressed by D2 Receptor activation. (A) Coronal slice, injection site of AAV-Chronos/tdTomato into GPe. (B) Photo-evoked GPe mediated IPSCs recorded in whole cell configuration from SNr neurons. (C) Paired T-test of photo-evoked IPSC amplitudes before and after bath application of 2 μM quinpirole; n = 5, p = 0.02. (D) Paired Pulses of GPe-mediated IPSCs at 50 ms interval before and after quinpirole bath application. (E) Paired T-test of paired pulse ratio of GPe-mediated IPSCs before and after quinpirole application; n = 6, p = 0.02

Figure 2. **Train stimulation of GPe input inhibits SNr spiking.** (A) A 6 second cell attached recording of SNr spiking inhibited by a 2 sec 20 Hz train stimulation of GPe-mediated IPSCs, before and after bath application by quinpirole. (B) A 6 second PSTH of cell attached spiking inhibited by a 2 sec 20 Hz train stimulation of GPe-mediated IPSCs, before and after bath application of quinpirole. (C) Wilcoxon matched-pairs signed rank test of percent inhibition (change in discharge rate / basal discharge rate) before and after quinpirole, n = 8, p = 0.02

Figure 3. GABA-A receptor blockade occludes disinhibition by quinpirole. (A) Example trace and summary data of cell attached spiking from SNr neurons before and after bath application of quinpirole. Paired T-test, n = 8, p < 0.01. (B) Example trace and summary data of cell attached spiking from SNr neurons before and bath application of gabazine. Paired T-test, n = 10, p < 0.01. (C) Example trace and summary data of cell attached spiking from SNr neurons pretreated with gabazine, before and after bath application of quinpirole. Paired T-test, n = 7, p = 0.06. (D) Hypothesized schematic of cells in SNr and SNc, showing the expression of D1 and D2 receptors that could be modulating GABA release upon SNr neurons.

Figure 4. Inhibition of GPe input does not alter tonic spiking in SNr. GPe injected with inhibitory Gi-DREADDs. (A) Example trace and summary data of electrically evoked GPe-mediated IPSCs before and after bath application of DREADD agonist CNO. Paired T-test, n = 4, p = 0.02. (B) Example trace and summary data of cell attached spiking from SNr neurons before and after bath application of CNO. Paired T-test, n = 5, p = 0.19

Figure 5. Astrocyte modulation of SNr spiking is unrelated to Tonic GABA (A) Schematic of Gq-DREADD expression in Astrocytes. CNO application triggers intracellular calcium release and

modulates conductance of bestrophin 1 channels. (B) Example trace and summary data of cell attached spiking from SNr neurons before and after bath application of DREADD agonist CNO. Paired T-test, n = 8, p = 0.03. (C) Example trace and summary data of cell attached spiking from SNr neurons before and after bath application of BST1 antagonist NPPB. Paired T-test, n = 6, p = 0.03.

Figure 6. Blockade of ALDH1A1 disrupts tonic GABA in SNr. (A) Coronal image of DAT-Cre+ / ALDH1A1+ (green) and DAT-Cre+ / ALDH1A1- (red) neurons in rostral substantia nigra. (B) Coronal image of DAT-Cre+ / ALDH1A1+ (green) and DAT-Cre+ / ALDH1A1- (red) neurons in caudal substantia nigra. (C) Coronal image of ALDHA1-shRNA-mCherry expression in SNc. (D) Example trace and summary data of cell attached spiking from control SNr neurons, and SNr neurons from animals injected with ALDH-shRNA. Welch's T-test, n = 18 control/15 shRNA, p < 0.001. (E) Example trace and summary data of cell attached SNr neuron spiking from mice injected with ALDH-shRNA before and after bath application with gabazine. Paired T-test, n = 15, p = 0.10. (F) Example trace and summary data of SNr spiking from control neurons and neurons pretreated with ALDH1A1 antagonists DEAB or disulfiram. Welch's T-test, n = 18 control/18 blocked, p = 0.01. (G) Example trace and summary data of SNr spiking pretreated with DEAB, before and after bath application of gabazine. Paired T-test, n = 5, p = 0.19. (H) Example trace and summary data of SNr spiking pretreated with disulfiram, before and after bath application of gabazine. Paired T-test, n = 5, p = 0.80.

Figure 7. Chemogenetic inhibition of SNc disinhibits SNr. (A) 10X image of substantia nigra of a DAT-Cre mouse. TH labelled with Rb-anti TH 488. DAT-Cre+ dopamine neurons infected with AAV9-Ef1a-DIO-PSAM-L141F-Y115F-GlyR-2A-FusionRed. (B) 60X image of substantia nigra, TH is green, PSAM-GlyR is red. (C) Schematic of PSEM agonist activating chloride influx into SNc neurons; hyperpolarization reduces GABA efflux from SNc neurons. (D) Example trace and summary data of SNc neurons infected with PSAM-GlyR before and after bath application of PSEM agonist uPSEM817 tartate. Summary data shows change in rate from SNc neurons after bath application of PSEM agonist, n = 10. (E) Example trace and summary data of SNr neuron spiking from PSAM-GlyR infected mice before and after bath application of PSEM agonist. Paired T-test, n = 8, p = 0.02.

Figure 8. Tonic GABA is lost in dopamine depleted MC1-Park mice. (A) Example trace and summary data of SNr neurons from MCI-Park- mice before and after bath application of gabazine.

(B) Example trace and summary data of SNr neurons from P60 – P70 MC1-Park+ mice before and after bath application of gabazine. Paired T-test, n = 7, p = 0.69.

Figure 9. Revised Schematic for Corelease of DA and GABA in SNr. Quinpirole acts upon SNc D2 autoreceptors to inhibit GABA and DA release in the SNr. Reduced tonic GABA disinhibits SNr neurons and enhances firing rate. In addition, reduced DA release dis-facilitates GABA release from dSPN terminals onto SNr neurons, also enhancing SNr firing rate. GPe inputs and astrocytes appear unrelated to tonic GABA inhibition, while astrocytes potentially contribute a tonic excitation of SNr neurons.

Supplemental Figures:

Figure S1. D1R antagonist significantly elevates SNr spike rate. Example trace and summary data of cell attached spiking from SNr neurons before and after bath application of SCH39166. Paired T-test, n = 12, p = 0.02.

Figure S2. Deletion of ALDH1A1 does not affect basal dopamine release. (A) Schematic of the FSCV experiment in coronal striatal slices. Inset: 2D voltammogram showing oxidation and reduction peaks of DA. (B) Representative 3D voltammograms from paired pulse stimulation; x axis: recording time; y axis: applied potential; color map: recorded current. (C-D) Quantification of peak DA release evoked by 1-pulse (C) and 5-pulse (D) stimulation. 1 pulse data are from the first pulse of the paired pulse represented by (B). (E) Quantification of the 15s ISI paired pulse ratio represented by (B).

Figure 1. Optically Evoked GPe mediated IPSCs are depressed by D2 Receptor activation.

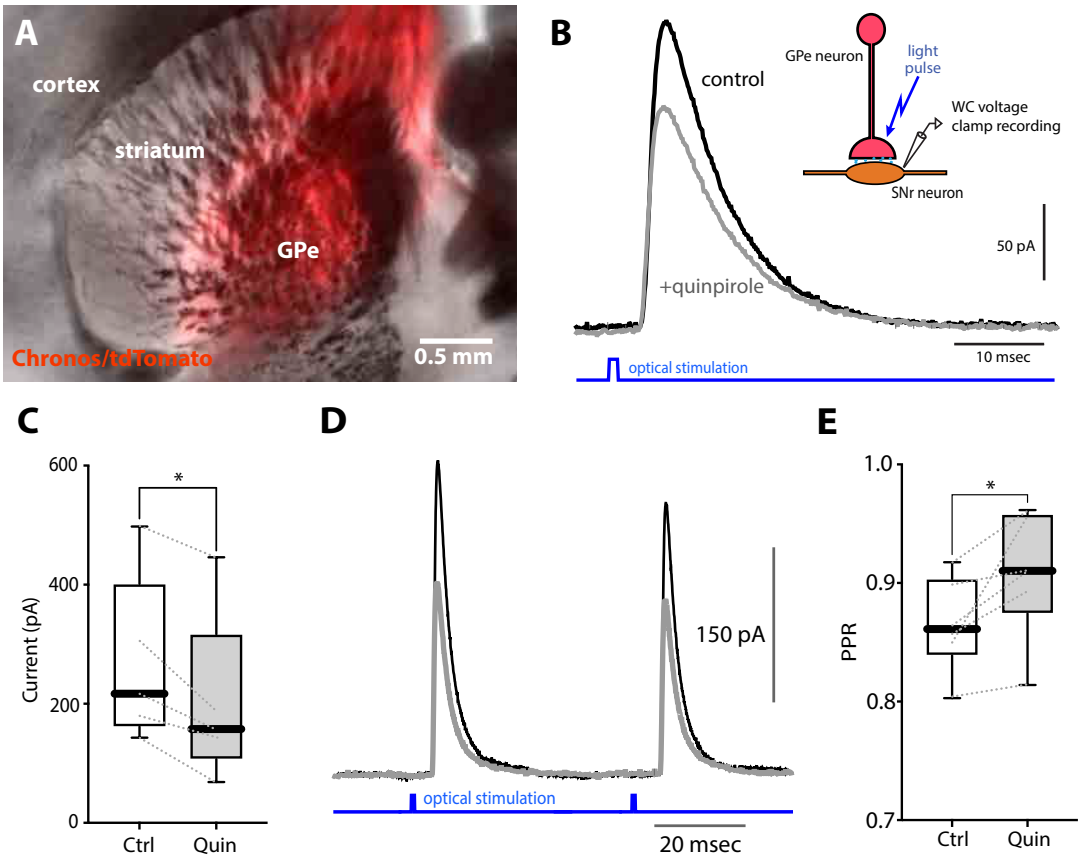

Figure 2. Train stimulation of GPe input inhibits SNr spiking.

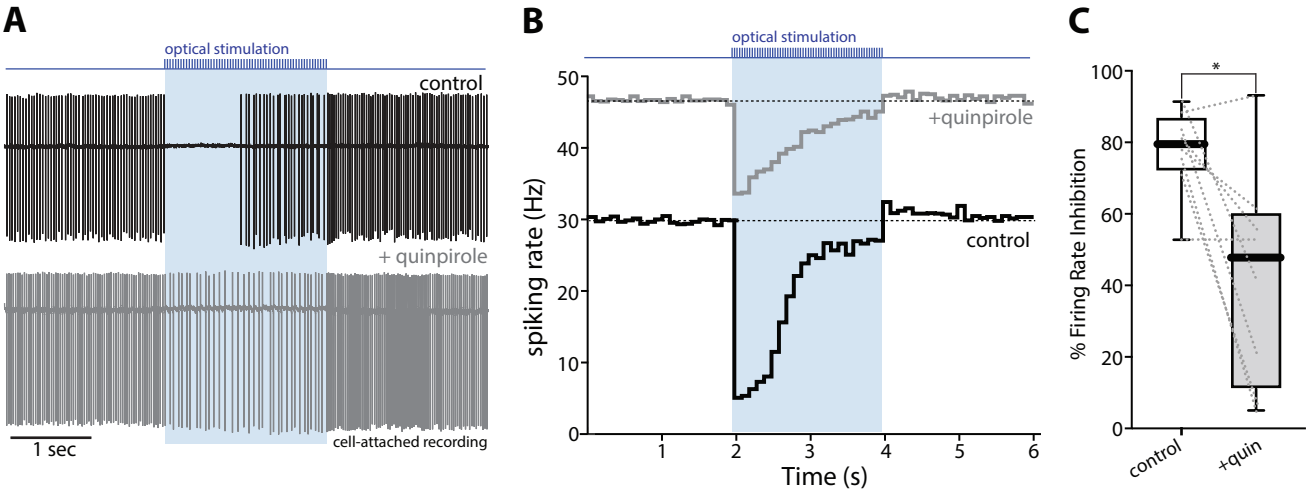

Figure 3. GABA-A receptor blockade occludes disinhibition by quinpirole.

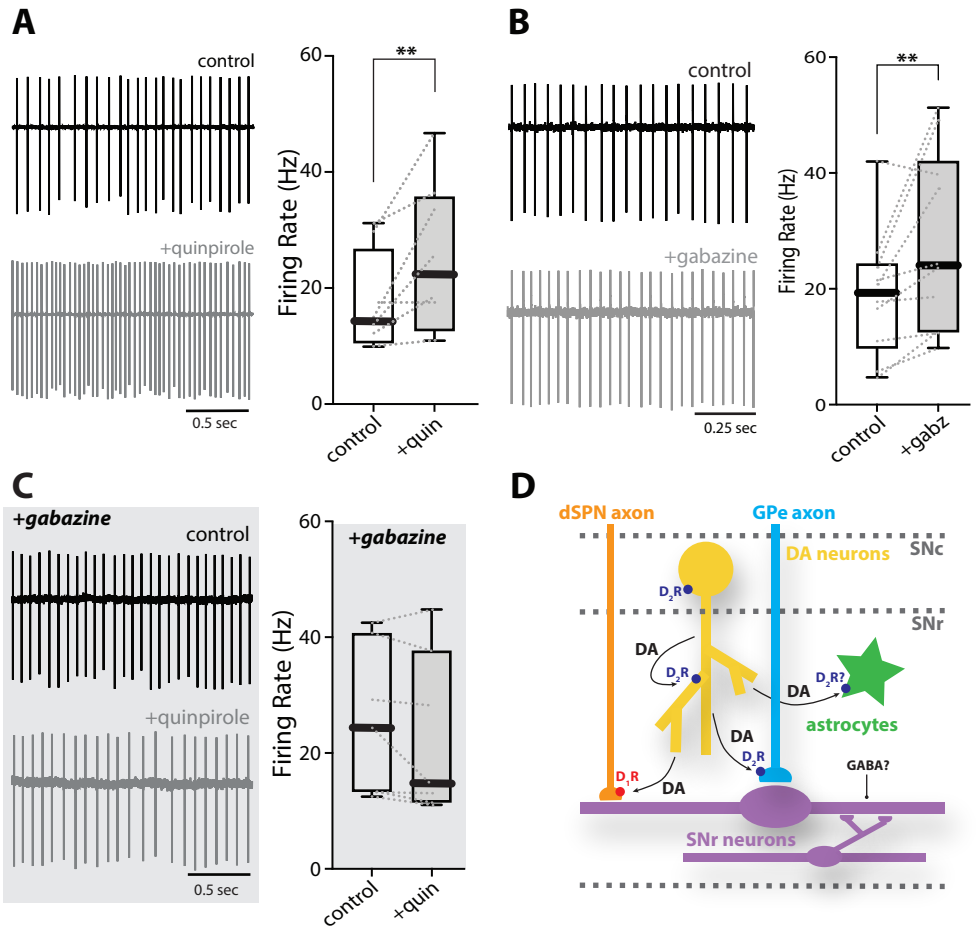

Figure 4. Inhibition of GPe input does not alter tonic spiking in SNr.

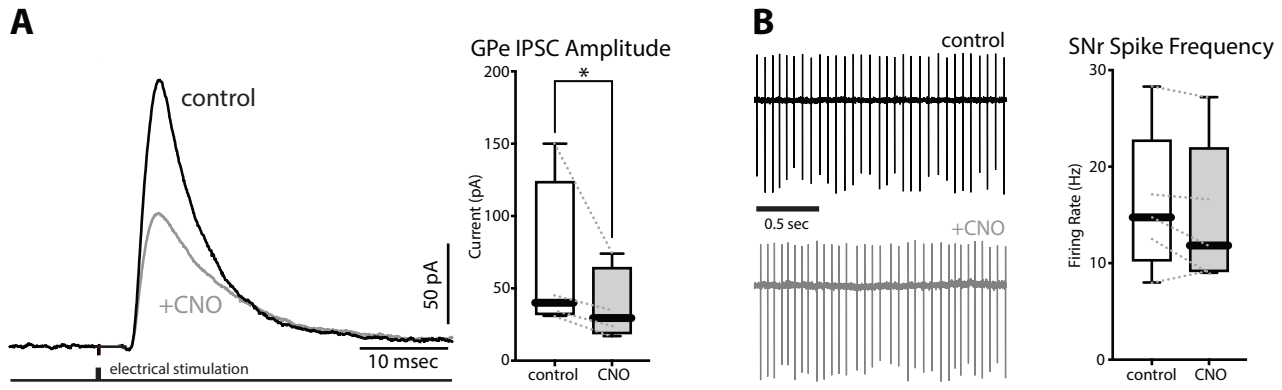

Figure 5. Astrocyte modulation of SNr spiking is unrelated to Tonic GABA

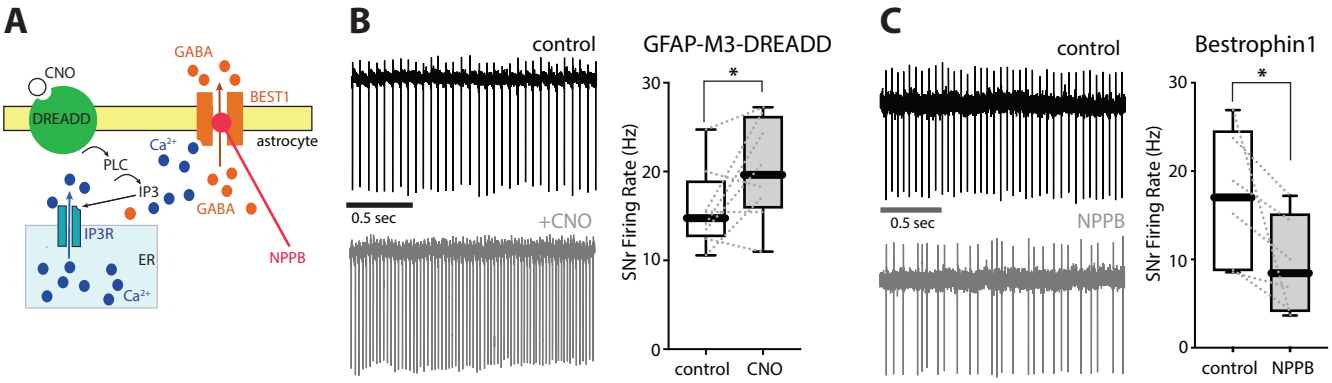

Figure 6. Blockade of ALDH1a1 disrupts tonic GABA in SNr.

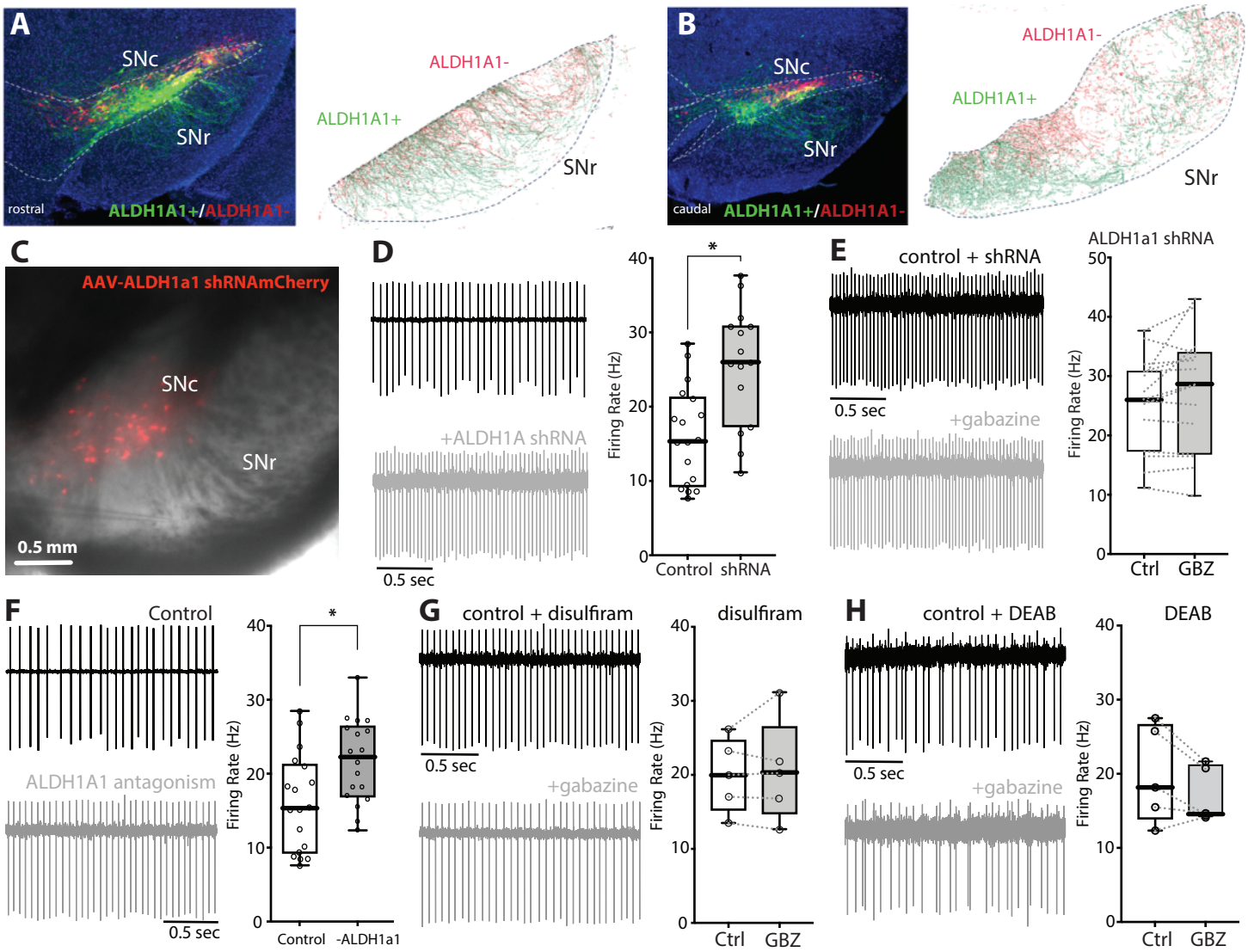

Figure 7. Chemogenetic inhibition of SNc disinhibits SNr.

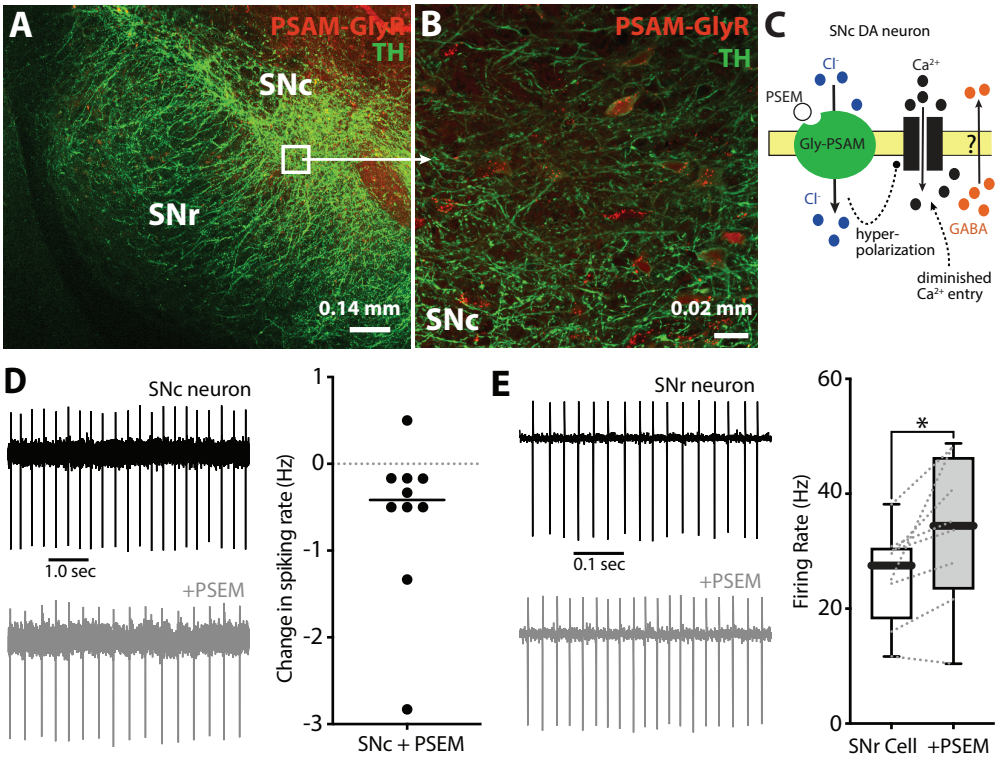

Figure 8. Tonic GABA is lost in dopamine depleted MC1-Park mice.

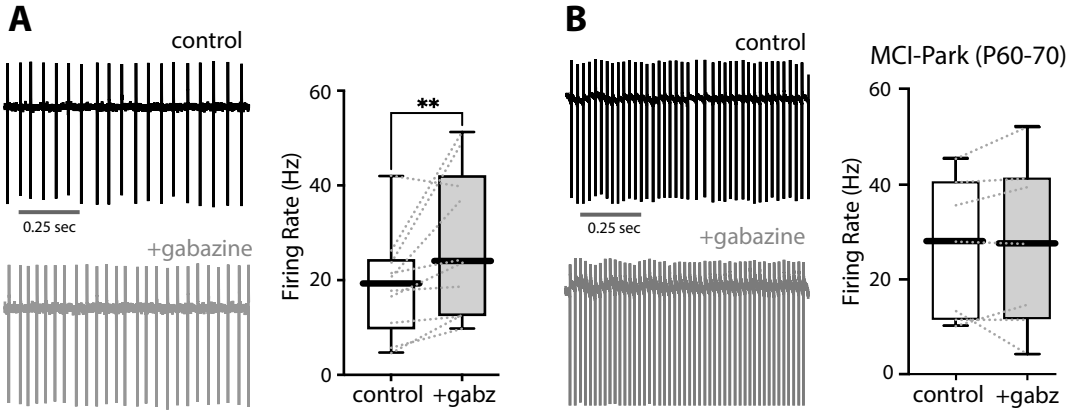

Figure 9. Revised Schematic for Corelease of DA and GABA in SNr.

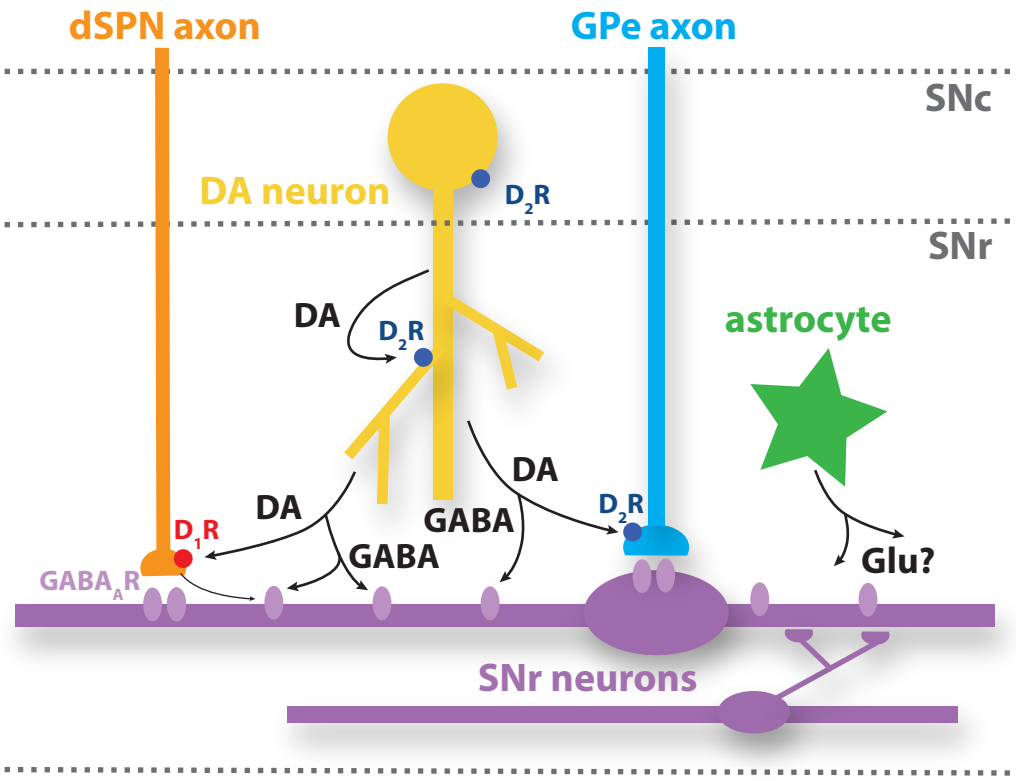

Supplementary Figure 1. D1R antagonist significantly elevates SNr spike rate.

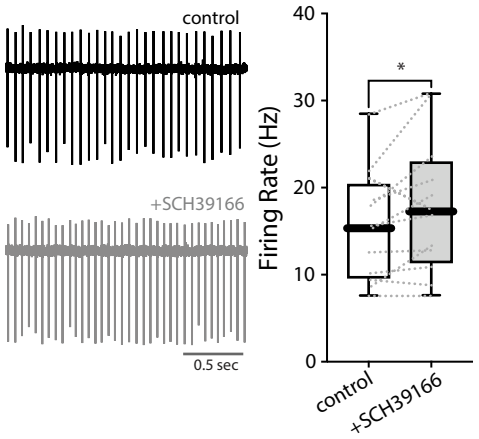
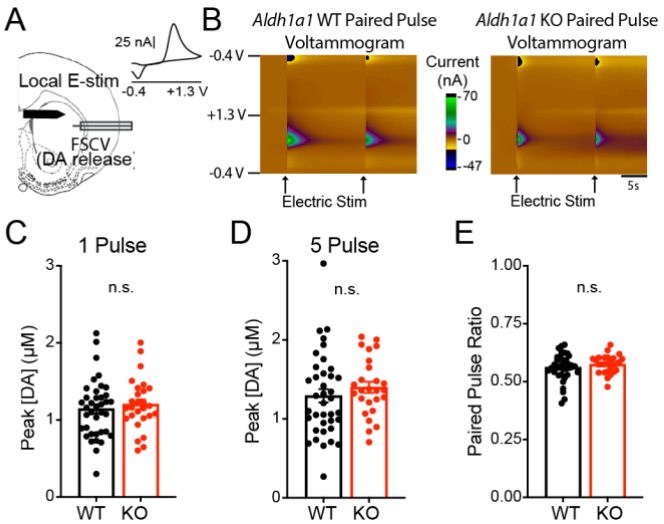
Supplementary Figure 2. Deletion of ALDH1A1 does not impact dopamine release.